SAND2014-18636C

Computational Stochastic Mechanics–Proc. of the 7th International Conference (CSM-7)
G. Deodatis and P.D. Spanos (eds.)
Santorini, Greece, June 15–18, 2014

ON-THE-FLY GENERATION OF SAMPLES OF NON-STATIONARY GAUSSIAN PROCESSES

R. V. FIELD, JR.[1] and M. GRIGORIU[2]

[1] *Sandia National Laboratories, USA. E-mail: rvfield@sandia.gov*
[2] *Cornell University, USA. E-mail: mdg12@cornell.edu*

A Monte Carlo algorithm is developed for generating samples of real-valued non-stationary Gaussian processes. The method is based on a generalized version of Shannon's sampling theorem for bandlimited deterministic signals, as well as an efficient algorithm for generating conditional Gaussian variables. One feature of the method that is attractive for engineering applications involving stochastic loads is the ability of the algorithm to be implemented "on-the-fly" meaning that, given the value of the sample of the process at the current time step, it provides the value for the sample of the process at the next time step. Theoretical arguments are supported by numerical examples demonstrating the implementation, efficiency, and accuracy of the proposed Monte Carlo simulation algorithm.

Keywords: Monte Carlo simulation, on-the-fly sample generation, sampling theorem, stochastic processes.

1 Introduction and Motivation

Current algorithms for generating samples of non-stationary Gaussian processes are based on Cholesky decompositions (Franklin, 1965), Karhunen-Loève representations (Grigoriu, 2002, Section 3.9.4.4, Hernández, 1995, Section 6.2), Fourier series representations with Gaussian coefficients (Grigoriu, 2002, Section 5.3.2.2), a generalized version of the spectral representation theorem (Grigoriu, 2010), and filtered Gaussian processes (Grigoriu, 2002, Section 5.3.2.1). Although these representations are general, their construction can be time consuming and usually involves technicalities. For example, the implementation of a Monte Carlo algorithm based on the Karhunen-Loève expansion involves the calculation of the eigenfunctions and eigenvalues of an integral operator with kernel equal to the correlation function of the target process.

Simple representations of non-stationary Gaussian processes are available in special cases, for example, stationary Gaussian processes modulated by deterministic functions, stationary Gaussian processes with distorted time scale (Grigoriu, 2003), Gaussian processes whose harmonics have amplitudes varying slowly in time, also referred to as oscillatory processes (Priestley, 1965), and Gauss-Markov processes defined by differential or finite difference equations driven by Gaussian white noise (Grigoriu, 2001).

Our objective is to develop a Monte Carlo algorithm for generating non-stationary Gaussian samples that is: (1) general, that is, it can be applied to generate samples of arbitrary non-stationary Gaussian processes; (2) accurate, that is, estimates obtained from samples produced by the algorithm match properties of target non-stationary Gaussian processes; and (3) efficient, that is, the algorithm can be implemented simply and its use is not computationally demanding. To address item (2), we provide a detailed analysis of errors associated with the practical use of the algorithm for sample generation, including the effects of truncation and aliasing. We note that while the aliasing error for stationary Gaussian processes has been studied previously by Gardiner (1972), we herein provide a bound on the aliasing error for non-stationary Gaussian processes that appears to be a new result.

Item (3) is of particular interest when the stochastic process being sampled serves as input to a dynamic system represented by a complex finite element (FE) model; applications include wind loads on civil engineering structures and aerodynamics forces on aerospace vehicles. The traditional approach is to calculate realizations of the applied loads for the entire time record of interest independent of the transient dynamics calculations of the FE solver. Hence, it is necessary to store the realizations of the load to a file for later application as input to the finite element model, which can become infeasible for large models and/or simulations of long dynamic events. To illustrate, consider the structural response of a spacecraft to external aerodynamic forces, *e.g.*, planetary entry, that vary in time and space. An analysis of this event would require time-varying pressure loads for each finite element modeling the outside surface of the spacecraft; the resulting data file could require terabytes of disk space for storage. The proposed method instead calculates realizations of the load over a small time window which moves as the simulation progresses. When embedded within a transient dynamics solver, the load can be computed "on-the-fly" meaning that, given the value of the load at the current time step, it provides the load at the next time step only. No external data file is needed for storage. This approach can be very useful for dynamic simulations of large models and/or when many time points are needed.

The organization of this paper is as follows. The accuracy of approximations based on the sampling theorem is discussed in detail in Section 2, and details on the implementation and its efficiency are provided in Section 3. Examples are provided in Section 4 to illustrate these features.

2 The Sampling Theorem and its Accuracy

Let $x(t)$, $t \in \mathbb{R}$, be a real-valued deterministic *bandlimited* function, *i.e.*, the frequency content of $x(t)$ is contained entirely within frequency band $(-\nu_c, \nu_c)$, $0 < \nu_c < \infty$. Let

$$x_n(t) = \sum_{|k| \leq n} x(k\,t_c)\,\alpha(t - k\,t_c), \qquad (1)$$

for $n = 1, 2, \ldots$, define a sequence of approximations for $x(t)$, where $\alpha(t) = \sin(\nu_c\,t)/(\nu_c\,t)$, $t \in \mathbb{R}$, and $t_c = \pi/\nu_c$. Because $\alpha((q - r)\,t_c) = 0$ for $q \neq r$ and 1 for $q = r$, we have that $x_n(t) = x(t)$ at $t = k\,t_c \leq n\,t_c$. The Shannon sampling theorem states that $x_n(t)$ defined by Eq. (1) converges to $x(t)$ as $n \to \infty$ at each $t \in \mathbb{R}$ (Papoulis, 1977, Section 5-1).

It is common in applications to approximate x by x_n defined by Eq. (1) with $n < \infty$; there are two types of errors associated with this approximation, referred to as *truncation error* and *aliasing error*. A bound for the truncation error, defined as $e_n(t) = |x(t) - x_n(t)|$, is available in Papoulis (1966) for $|t| < n\,t_c$, and can be made as small as desired by increasing the value for n.

Let $\bar{\nu} > 0$ be an arbitrary frequency, referred to as the sampling frequency, and let $\bar{x}_n$ be x_n in Eq. (1) with $\bar{t} = \pi/\bar{\nu}$ in place of t_c. If $\bar{\nu} \geq \nu_c$, then $x(t) = \lim_{n\to\infty} \bar{x}_n(t)$ at each $t \in \mathbb{R}$ and there is no aliasing error. If $\bar{\nu} < \nu_c$, then aliasing occurs and $\bar{x}_\infty(t) = \lim_{n\to\infty} \bar{x}_n(t)$ does not coincide with $x(t)$. The difference $e_a(t) = |x(t) - x_\infty(t)|$, referred to as aliasing error, can be bounded by

$$e_a(t) \leq \frac{1}{\pi} \int_{|\nu|>\bar{\nu}} |x_F(\nu)| \, \mathrm{d}\nu, \qquad (2)$$

provided that $x_F(\nu)$, the Fourier transform of $x(t)$, is absolutely integrable (Brown 1967; Jerri, 1977). By Eq. (2), we note that the aliasing error decreases with increasing $\bar{\nu}$.

In the following sections, we review extensions of the sampling theorem described above to the case of stationary and non-stationary Gaussian stochastic processes, and provide some discussion on the associated truncation and aliasing errors that occur. Numerical examples are presented to illustrate the effects of these errors.

2.1 *Sampling Theorem for Stationary Processes*

Let $X(t)$, $t \in \mathbb{R}$, be a stationary Gaussian stochastic process with zero mean, covariance function $c(\tau) = \mathrm{E}[X(t+\tau)\,X(t)] = \int_{\mathbb{R}} e^{i\,\nu\,\tau}\, s(\nu)\,\mathrm{d}\nu$, and spectral density $s(\nu) = (2\pi)^{-1} \int_{\mathbb{R}} e^{-i\,\nu\,\tau}\, c(\tau)\,\mathrm{d}\tau$, where $i = \sqrt{-1}$. The process is defined on a probability space $(\Omega, \mathcal{F}, P)$, and we use notation $X(t,\omega)$, $\omega \in \Omega$ to refer to a particular sample of X.

Our objective in this section is to apply the Shannon sampling theorem to approximate $X(t)$; the following two subsections deal with processes $X(t)$ whose spectral densities have bounded and unbounded support.

2.1.1 *Bandlimited Processes*

Suppose $X(t)$ is a bandlimited process with bandwidth $(-\nu_c, \nu_c)$, $0 < \nu_c < \infty$, *i.e.*, its spectral density satisfies $s(\nu) = 0$ for $|\nu| > \nu_c$. Let

$$X_n(t) = \sum_{|k|\leq n} X(k\,t_c)\,\alpha(t - k\,t_c), \qquad (3)$$

for $n = 1, 2, \ldots$, be a sequence of processes with the notation introduced by Eq. (1). The approximations X_n for X defined by Eq. (3) are referred to as *global representations* (Grigoriu, 1993). It can be shown that: (i) the second moment properties of X_n converge to those of X as $n \to \infty$, so that X_n becomes a version of X as n increases since X and X_n are both Gaussian processes; (ii) the sequence $\{X_n(t)\}$ of random variables converges to $X(t)$ in the mean square (m.s.) sense as $n \to \infty$, that is, $\lim_{n\to\infty} \mathrm{E}[(X(t) - X_n(t))^2] = 0$ at any time t; and (iii) X_n converges almost surely (a.s.) to X as $n \to \infty$ (Belyaev, 1959; Grigoriu, 1993).

It can be shown that these properties also hold for the sequence of processes defined by

$$\tilde{X}_n(t) = \sum_{k=n_t-n}^{n_t+n+1} X(k\,t_c)\,\alpha(t - k\,t_c), \qquad (4)$$

for $t \in [n_t\,t_c, (n_t+1)\,t_c]$, where $n_t = \lfloor t/t_c \rfloor$ is the largest integer smaller than t/t_c (Grigoriu, 1993). The representation $\tilde{X}_n$ defined by Eq. (4), referred to as a *local representation* for X, is particularly useful for calculations since its values in time cell $[n_t\,t_c, (n_t+1)\,t_c]$ depend on values of X at only $2\,(n+1)$ times, that is, at the nodal time points $\{k\,t_c\}$, $k = n_t - n, \ldots, n_t + n + 1$. In contrast, the number of terms needed for the global representation defined by Eq. (3) increases with $|t|$ and becomes very large for $|t| \gg 0$. It is this feature of the local representation that facilitates efficient on-the-fly generation of samples of $\tilde{X}_n(t)$ discussed in Section 1.

For bandlimited processes, there can be no aliasing error as long as the sampling frequency is strictly larger than ν_c. Let $\mathcal{E}_n(t) = |X(t) - X_n(t)|$ and $\tilde{\mathcal{E}}_n(t) = |X(t) - \tilde{X}_n(t)|$ define the truncation errors associated with the global and local representations for X defined by Eqs. (3) and (4), respectively. Because X, X_n, and $\tilde{X}_n$ are stochastic processes, so too are the errors $\mathcal{E}_n(t)$ and $\tilde{\mathcal{E}}_n(t)$. The truncation errors can be bounded by using arguments similar to those used to derive the bound for deterministic functions (Papoulis, 1966), but the resulting bounds are of limited use for applications since they are complex functionals of X and their probability law cannot be obtained analytically. For example, the bound (Helms and Thomas, 1962)

$$\tilde{\mathcal{E}}_n(t) \leq \frac{4}{\pi^2 n} \max_t \{|X(t)|\} \qquad (5)$$

is valid for processes with a.s. finite energy.

2.1.2 *Non-Bandlimited Processes*

Next suppose that the spectral density of $X(t)$ does not have a bounded support. Let $\nu_c > 0$ be a finite but otherwise arbitrary cutoff frequency, and let X_n and $\tilde{X}_n$ be the processes defined by Eqs. (3) and (4), *i.e.*, the global and local representations for X, respectively. The magnitude of the differences between these representations and the target process X depend on the values for $n < \infty$ (truncation error) and $\nu_c < \infty$ (aliasing error).

It is possible to develop bounds on both truncation and aliasing errors for the case of non-bandlimited processes. For example, an upper bound related to the aliasing error is given by (Brown, 1978)

$$\begin{aligned} \varepsilon_a(t) &= \lim_{n\to\infty} \mathrm{E}\left[(X(t) - X_n(t))^2 \right] \\ &\leq \frac{1}{\pi} \int_{|\nu|>\nu_c} s(\nu)\, \mathrm{d}\nu, \end{aligned} \qquad (6)$$

where $s(\nu)$ is the spectral density of $X(t)$. This bound constitutes a special case of the bound for non-stationary processes established in the following section (see Eq. (12)). This bound demonstrates that the accuracy of X_n depends on the energy of X outside the frequency band $(-\nu_c, \nu_c)$, as expected.

2.2 *Sampling Theorem for non-Stationary Processes*

Let $X(t)$, $t \in I \subset \mathbb{R}$, be a real-valued non-stationary Gaussian processes with zero mean, finite variance, and covariance function $c(s,t) = \mathrm{E}[X(s)\, X(t)]$. The generalized spectral density of X and the covariance function of this process are double Fourier pairs, that is

$$s(\nu,\eta) = \frac{1}{(2\pi)^2} \int_{\mathbb{R}^2} c(s,t)\, e^{-i\,(\nu\, s - \eta\, t)}\, \mathrm{d}s\, \mathrm{d}t, \qquad (7)$$

and

$$c(s,t) = \int_{\mathbb{R}^2} s(\nu,\eta)\, e^{i\,(\nu\, s - \eta\, t)}\, \mathrm{d}\nu\, \mathrm{d}\eta. \qquad (8)$$

Note that the generalized spectral density $s(\nu,\eta)$ in Eq. (7) exists if $c(s,t)$ is absolutely integrable in $\mathbb{R}^2$, that is, if $\int_{\mathbb{R}^2} |c(s,t)|\, \mathrm{d}s\, \mathrm{d}t < \infty$. Under this condition, we have $(2\pi)^2\, |s(\nu,\eta)| \leq \int_{\mathbb{R}^2} |c(s,t)|\, |e^{-i\,(\nu\, s - \eta\, t)}|\, \mathrm{d}s\, \mathrm{d}t = \int_{\mathbb{R}^2} |c(s,t)|\, \mathrm{d}s\, \mathrm{d}t$, which is finite by assumption.

In the reminder of this section we give properties of the generalized spectral density $s(\nu,\eta)$ that are relevant to our discussion; the properties are utilized in Section 4 to ensure all example spectral densities considered are indeed valid. We include processes whose spectral densities have, or do not have, bounded support.

Prop 2.1 The generalized spectral density is complex-valued even for real-valued processes and satisfies $s(\nu,\eta)^* = s(\eta,\nu)$ for all $\nu, \eta \in \mathbb{R}$. The spectral ordinates $s(\nu,\nu)$ are real-valued.

Proof. The proof can be found in Field *et al.*, (2013). □

As a consequence of Property 2.1, the real and imaginary parts of the generalized spectral densities are such that $\mathrm{Re}[s(\nu,\eta)] = \mathrm{Re}[s(\eta,\nu)]$ and $\mathrm{Im}[s(\nu,\eta)] = -\mathrm{Im}[s(\eta,\nu)]$.

Prop 2.2 If X is a weakly stationary process with zero mean, covariance function $c_0(s-t) = \mathrm{E}[X(s)\,X(t)]$ and spectral density s_0, its generalized spectral density is

$$s(\nu,\eta) = s_0\left(\frac{\nu+\eta}{2}\right)\delta(\nu-\eta), \quad (9)$$

that is, the entire energy of the process is concentrated in the subset $\{(\nu,\eta) : \nu = \eta\}$.

Proof. The proof can be found in Field *et al.*, (2013). □

2.2.1 *Bandlimited Processes*

Let $X(t)$, $t \in \mathbb{R}$, be a real-valued, non-stationary process with zero mean and generalized spectral density with bounded support, *i.e.*, $s(\nu,\eta)$ defined by Eq. (7) satisfies

$$s(\nu,\eta) = 0, \quad (\nu,\eta) \in D^c, \quad (10)$$

where $D = [-\nu_c,\nu_c] \times [-\nu_c,\nu_c]$ and $0 < \nu_c < \infty$ is a constant. Let $X_n(t)$ be the approximation for $X(t)$ defined by Eq. (3). As discussed previously, there is no aliasing error for bandlimited processes, but we have the following result related to the truncation error for this case.

Theorem 2.1 *The m.s. difference between $X(t)$ and its representation $X_n(t)$ is such that*

$$\lim_{n\to\infty} E\left[\left(X(t) - \sum_{k=-n}^{n} X(k\,t_c)\,\alpha(t-k\,t_c)\right)^2\right] = 0. \quad (11)$$

Proof. The proof of the m.s. convergence in Eq. (11) can be found in Gardiner (1972). □

Remark 2.1 This result demonstrates that the sampling theorem representation defined by Eq. (3) can also be used to approximate bandlimited non-stationary processes. As for stationary processes, we can derive bounds on the truncation error, that is, on the expectation in Eq. (11) for specified values of truncation level n.

2.2.2 *Non-Bandlimited Processes*

Let $X(t)$ be a non-stationary process with zero mean and generalized spectral density $s(\nu,\eta)$ that does not have a bounded support. In this case, we can show that the sampling theorem representation X_n defined by Eq. (3) corresponding to an arbitrary cutoff frequency $0 < \nu_c < \infty$ can be used to approximate X under some conditions. The quality of the approximation X_n depends on the values of n (truncation error) and ν_c (aliasing error). The local representation in Eq. (4) has similar properties.

Theorem 2.2 *If $s(\nu,\eta)$ is square integrable, that is, if $\int_{\mathbb{R}^2} |s(\nu,\eta)|^2\,\mathrm{d}\nu\,\mathrm{d}\eta < \infty$, then*

$$\varepsilon_a(t) = \lim_{n\to\infty} E\left[(X(t) - X_n(t))^2\right] \le 4\int_{D^c} |s(\nu,\eta)|^2\,\mathrm{d}\nu\,\mathrm{d}\eta. \quad (12)$$

Proof. The proof can be found in Field *et al.*, (2013). □

Remark 2.2 By Theorem 2.2, the mean square value of the aliasing error defined in Section 2.1.1 is bounded by the volume of the absolute value of the generalized spectral density of X in D^c. We note that the requirement $\int_{\mathbb{R}^2} |s(\nu,\eta)|\,\mathrm{d}\nu\,\mathrm{d}\eta < \infty$ is stronger than $X \in L^2$ since, if $s(\nu,\eta)$ is absolutely integrable, then $c(t,t) \le \int_{\mathbb{R}^2} |s(\nu,\eta)|\,\mathrm{d}\nu\,\mathrm{d}\eta < \infty$ implying $X \in L^2$.

Remark 2.3 The bound in Eq. (12) is similar to that in Eq. (6) for weakly stationary non-bandlimited processes. Theorem 2.2 is an analogue, not a generalization, of Eq. (6). We note that the difference between the coefficients in front of the bounds relates to the differences between the Fourier pairs in Eqs. (7) and (8), and the relationship $c(\tau) = \int_{-\infty}^{\infty} s(\nu)\, e^{i\,\nu\,\tau}\, \mathrm{d}\nu/(2\,\pi)$ used in Brown (1978) to establish the bound in Eq. (6).

3 Implementation of the Sampling Theorem

Let $X(t)$ be a non-stationary Gaussian process with zero mean, covariance function $c(s,t) = \mathrm{E}[X(s)\,X(t)]$, and generalized spectral density $s(\nu,\eta)$ defined by Eq. (7). Our objective in this section is to develop an efficient procedure to generate independent samples of $X(t)$ in a time interval $t \in [0, \tau = n_c\, t_c]$, where $n_c \geq 1$ is an integer.

The generation of samples of $X(t)$ can be based on the following three step algorithm that uses the local representation $\tilde{X}_n$ of X defined by Eq. (4). Samples of X_n and $\tilde{X}_n$ can be used as substitutes for samples of X since the second moment properties of these approximate representations converge to those of X as $n \to \infty$ and $\nu_c \to \infty$, and X_n, $\tilde{X}_n$, and X are all Gaussian processes. We first generate samples of $\tilde{X}_n$ in the time interval $[0, t_c]$ and then extend these samples over successive time intervals.

(1) Select a cutoff frequency $\nu_c > 0$ and a half window width n defining the number of nodal values $\{X(k\,t_c)\}$, $k = n_t - n, \ldots, n_t + n + 1$, needed to describe $X(t)$ within cell $t \in [n_t\, t_c, (n_t+1)\, t_c]$, where $n_t = \lfloor t/t_c \rfloor = \lfloor \nu_c\, t/\pi \rfloor$.

(2) Suppose, for example, that X is zero at negative times, that is, $X(t) = 0$ for $t \leq 0$. We generate independent samples of the $\mathbb{R}^{2\,(n+1)}$-valued Gaussian variable $\{X(k\,t_c)\}$, $k = 1, \ldots, 2\,(n+1)$, based on classical algorithms (Grigoriu, 2002, Section 5.2.1), and use them and Eq. (4) to calculate corresponding samples of $\tilde{X}_n$ in cells $[0, t_c], \ldots, [(n+1)\, t_c, (n+2)\, t_c]$. Nodal values of X for negative times are set equal to 0. Slight modifications of this step need to be implemented for different starting conditions.

(3) Extend the samples in the time interval $[0, (n+2)\, t_c]$ to the time interval $[(n+2)\, t_c, \tau]$ by using properties of conditional Gaussian variables and Eq. (4). Let t be such that $n_t \geq n + 2$ and let $\mathbf{Z}$ be an $\mathbb{R}^{2\,(n+1)+1}$-valued Gaussian variable with first coordinate $Z_1 = X(n_t + n + 2)$ and the rest of coordinates $\mathbf{Z}_2 = \big(X(n_t + n + 1), \ldots, X(n_t - n)\big)$. The conditional variable $Z_1 \mid \mathbf{Z}_2$ is Gaussian with mean $\boldsymbol{\gamma}_{12}\, \boldsymbol{\gamma}_{22}^{-1}\, \mathbf{Z}_2$ and variance $\gamma_{11} - \boldsymbol{\gamma}_{12}\, \boldsymbol{\gamma}_{22}^{-1}\, \boldsymbol{\gamma}_{12}'$, where γ_{11} is the variance of Z_1, $\boldsymbol{\gamma}_{12}$ denotes the covariance matrix of Z_1 and $\mathbf{Z}_2$, and $\boldsymbol{\gamma}_{22}$ is the covariance matrix of $\mathbf{Z}_2$ (Grigoriu, 2002, Section 2.11.5). Since samples of $\mathbf{Z}_2$ have been already generated, the probability law of the real-valued Gaussian variable $Z_1 \mid \mathbf{Z}_2$ is known and can be used to generate samples of this variable. The definition of $\tilde{X}_n$ and the samples of Z_1 and $\mathbf{Z}_2$ can be used to construct the corresponding sample of this process in the time interval $[n_t\, t_c, (n_t+1)\, t_c]$.

4 Applications

Three example applications are considered below to illustrate the effectiveness of the sampling-theorem based approach; the examples are constructed to demonstrate the accuracy and efficiency of the proposed Monte Carlo algorithm. First, we consider a uniformly modulated stationary Gaussian process and a fractional Brownian motion. These processes, presented as Examples 4.1 and

4.2 below, are selected since their second moment properties can be obtained simply and observations regarding the accuracy of our approach via the truncation and aliasing errors can be made. For Example 4.3, we consider a more realistic application by using the proposed algorithm to generate samples of non-stationary processes that represent dynamic loads applied to a complex aerospace system. This latter example is presented to further highlight the numerical efficiency of the approach by exploiting the "on-the-fly" load generation feature of the method.

Example 4.1

Let $Y(t)$, $t \in \mathbb{R}$, be a stationary Gaussian process with zero mean and covariance function $c_Y(\tau) = \mathrm{E}[Y(t+\tau)\,Y(t)] = \exp(-\lambda\,|\tau|)$, $\lambda > 0$, $\tau \in \mathbb{R}$, and let $\beta(t) \geq 0$ be a deterministic function. Then

$$X(t) = \beta(t)\,Y(t), \quad t \in \mathbb{R}, \qquad (13)$$

is a non-stationary Gaussian process with zero mean, covariance function $c(s,t) = \mathrm{E}[X(s)\,X(t)] = \beta(s)\,\beta(t)\,c_Y(s-t)$, and generalized spectral density

$$s(\nu,\eta) = \frac{1}{(2\,\pi)^2}\int_{\mathbb{R}^2} \beta(s)\,\beta(t)\,\times \\ e^{-\lambda\,|s-t|}\,e^{-i\,(\nu\,s-\eta\,t)}\,\mathrm{d}s\,\mathrm{d}t. \qquad (14)$$

By Eq. (13), $X(t)$ is a special type of non-stationary stochastic process referred to as a uniformly modulated process (Grigoriu, 2001).

Five samples of $X(t)$, generated using the Monte Carlo algorithm outlined in Section 3, are illustrated by Fig. 1 for $n = \nu_c = 10$. The mean and standard deviation functions of $X(t)$ and their estimates calculated from samples of $\tilde{X}_n$ with $(n = 10,\ \nu_c = 10)$ are denoted by the red line shown in Fig. 2.

As demonstrated by Fig. 2, the accuracy of the estimates for the mean and standard deviation functions do not

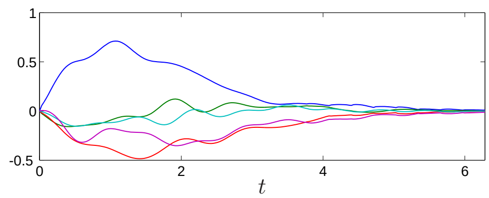

Fig. 1. Five samples of $X_n(t)$ defined by Example 4.1 for $n = 10$, and $\nu_c = 10$.

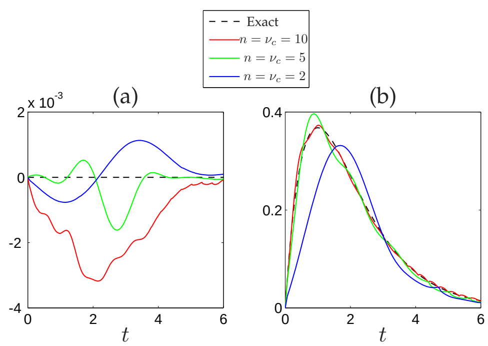

Fig. 2. Estimated and exact statistics of X for Example 4.1: (a) mean, and (b) standard deviation.

seem to be affected if both the truncation level n and the cutoff frequency ν_c are reduced from $(n = 10,\ \nu_c = 10)$ to $(n = 5,\ \nu_c = 5)$. That the reduction of the cutoff frequency from $\nu_c = 10$ to $\nu_c = 5$ does not decrease the accuracy of $\tilde{X}_n$ is expected since most of the power of the generalized spectral density of X is contained in the frequency band $[-5,5] \times [-5,5]$. However, a further reduction of the cutoff frequency ν_c yields unsatisfactory approximations $\tilde{X}_n$ of X, as demonstrated by the estimates of the second moment properties of X illustrated by Fig. 2 and obtained from 5000 independent samples of $\tilde{X}_n$ with $(n = 5,\ \nu_c = 2)$. The unsatisfactory performance of the representation $\tilde{X}_n$ considered here is caused by aliasing errors that are significant since only the frequency band $[-2,2] \times [-2,2]$ is considered and a significant portion of the power of X is outside this frequency band.

Example 4.2

Let $H \in (0,1)$ be a constant and let $B_H(t)$, $t \geq 0$, be a fractional Brownian motion, that is, a non-stationary Gaussian process with zero mean, covariance function

$$c_H(s,t) = \mathrm{E}[B_H(s)\, B_H(t)] = \frac{1}{2}\left[s^{2\,H} + t^{2\,H} - |s-t|^{2\,H}\right], \tag{15}$$

for $s,t \geq 0$, and initial state $B_H(0) = 0$. If $H = 1/2$, then B_H is a Brownian motion. If $H > 1/2$, then B_H has long range memory (Embrechts and Maejima, 2002).

Define, for $0 < \tau < \infty$,

$$X(t) = 1(0 \leq t \leq \tau)\, B_H(t), \tag{16}$$

where $1(\cdot)$ is the indicator function. The Monte Carlo simulation algorithm from Section 3 is applied to generate samples of X, that is, samples of B_H for $t \geq 0$, estimate second moment properties of B_H from its samples, and assess the accuracy of the estimated moments of B_H as a function of truncation level n and cutoff frequency ν_c. All numerical results are for $H = 0.7$, $\tau = 50$, and 5000 independent samples of $\tilde{X}_n$. Five samples of $X(t)$, generated using the Monte Carlo algorithm outlined in Section 3, are illustrated by Fig. 3 for $n = 10$.

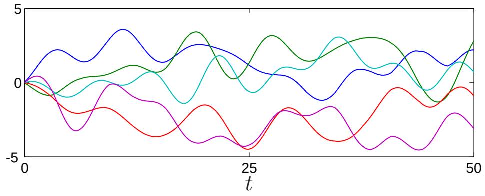

Fig. 3. Five samples of $X_n(t)$ defined by Example 4.2 for $n = 10$, and $\nu_c = 1$.

The exact covariance function $c(s,t)$ of $X(t)$ is illustrated by Fig. 4(a), while an estimate of this function obtained from 5000 samples of $\tilde{X}_n$ with $n = 10$ is illustrated by Fig. 4(b). The mean and standard deviation functions of $X(t)$ and their estimates calculated from samples of $\tilde{X}_n$ with $n = 10$ are denoted by the red line shown in Fig. 5. Similar results are illustrated for decreasing values of n. Estimates of the first two moments of X for truncation levels $n = 10$ and $n = 5$ have similar accuracy. However, estimates of these moments based on samples of $\tilde{X}_n$ with $n = 2$ are less accurate since small values for n result in large truncation errors. Aliasing errors are negligible in this case since most of the power of the generalized spectral density of X is included in the rectangle $[-\nu_c, \nu_c] \times [-\nu_c, \nu_c]$ for $\nu_c = 1$.

Example 4.3

The presence of time- and space-dependent random fluctuations in conditions within a planetary atmosphere, *e.g.*, temperature, density, and pressure, is a well-documented phenomenon (Jumper, *et al.*, 1997; Justus and Woodrum, 1990; Weill, *et al.*, 1976). For spacecraft structural design, it is often of interest to quantify the vibration response of the spacecraft and its internals to these fluctuations when undergoing ballistic entry (Gnoffo, *et al.*, 1998;Justus, *et al.*, 1990).

In Field, et al. (2011), the first author developed stochastic models for random fluctuations of air density and temperature within the Earth's atmosphere. When coupled with a trajectory analysis, these random fluctuations in atmospheric conditions can be mapped to a stochastic process that models spacecraft deceleration. Upon subtracting the mean deceleration and scaling by the vehicle mass, the resulting stochastic process represents a fluctuating drag force. This model for fluctuating drag force can be applied, for example, to a finite element (FE) model for an aerospace vehicle to

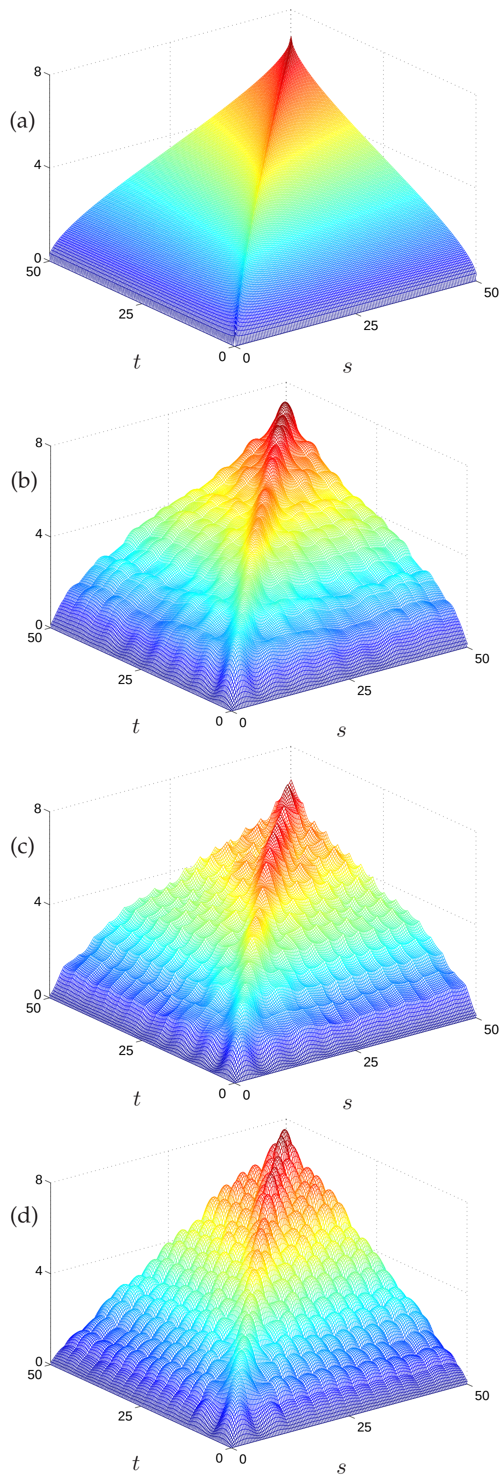

Fig. 4. Covariance functions for Example 4.2: exact (a), and estimates for the cases of $n = 10$ (b), $n = 5$ (c), and $n = 2$ (d).

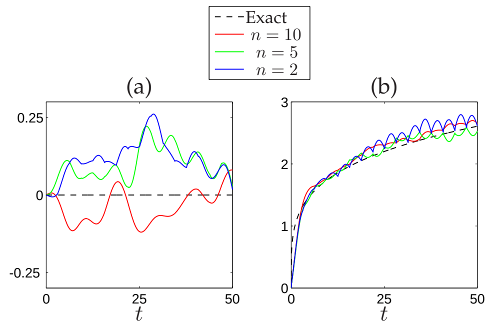

Fig. 5. Estimated and exact statistics of X for Example 4.2: (a) mean, and (b) standard deviation.

compute the resulting vibration response of internal components.

In this section, we utilize the proposed sampling-theorem based algorithm to provide an efficient and accurate framework for the analysis of the vibration response of a complex aerospace system subjected to the fluctuating drag force modeling random disturbances in atmospheric conditions. One possible application is the dynamic response of the Mars Pathfinder; a complex FE model of this system is discussed in Dieudonné and Spel (2004).

The traditional approach to this analysis is to calculate multiple independent realizations of the drag load over the entire entry event, store the realizations to a file, then read this file as input to a FE model for the spacecraft. It is not unusual for there to be tens of thousands of finite elements used to represent the outside surface of the spacecraft, and each element requires as input a time-varying load function defined for tens or hundreds of seconds. The resulting data files can be huge, rendering this approach infeasible for large FE models and/or simulations of long dynamic events. Instead, we utilize the proposed sampling-theorem based method, which calculates realizations of the load over a small time window which moves as the simulation progresses. When embedded within a transient dynamics solver, the load can be computed "on-the-fly" meaning that, given the value of the load at the current time step, it provides the load at the next time step only. No external data file is needed for storage.

Figure 6 illustrates 5 samples of $X(t)$, a non-stationary Gaussian process modeling fluctuating drag force applied to a finite element mesh of the Mars Pathfinder. These samples were taken directly from the simulation algorithm described in Field, et al. (2011), then scaled by the planetary entry mass. Process $X(t)$ is herein assumed to be Gaussian with zero mean for simplicity, but is non-stationary due to the inhomogeneity of the atmosphere and the changing speed of the spacecraft.

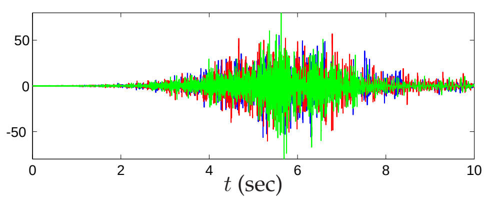

Fig. 6. Three samples of fluctuating drag force $X(t)$ in units of $\mathrm{lb_f}$ (taken from Field, et al. (2011)) considered for Example 4.3.

To utilize the proposed algorithm to create samples of the loading on the vehicle, all that is required is an estimate of $c(t,s) = \mathrm{E}[X(t)\,X(s)]$, the covariance function of the applied drag force. This estimate, based on 500 samples of $X(t)$ taken from Field, et al. (2011), is illustrated by Fig. 7; methods from Bendat and Piersol, (1986), Section 12.5.1, were used for the estimation procedure. The estimate of $c(t,s)$ is illustrated for four different time segments, each of length 0.1 seconds, in Fig. 7(a)–(d). In general, the frequency content of the signal decreases with increasing time, and the variance increases, then decreases with time. Both of these characteristics are further evidence of the non-stationarity of the drag force.

5 Conclusions

A new Monte Carlo algorithm was developed for generating samples of real-valued non-stationary Gaussian processes. To quantify the accuracy of the proposed approach, we analyzed in detail the truncation and aliasing errors associated with using the algorithm to produce samples of the target stochastic process. As a result, a new bound on the aliasing error for non-stationary Gaussian processes was developed. We also developed a new approach for the square-root-like decomposition of a sequence of covariance matrices that proved very beneficial for improving the overall computational efficiency of the algorithm. Further, it was demonstrated that the algorithm can be implemented "on-the-fly" meaning that, given the value of the sample of the process at the current time step, it provided the value for the sample of the process at the next time step. This feature proved attractive for engineering applications involving stochastic loads applied to complex finite element models since the realization of the load can be embedded within a transient dynamics solver, thereby eliminating the need for external storage of the load record.

Acknowledgement

Sandia National Laboratories is a multi-program laboratory managed and operated by Sandia Corporation, a wholly owned subsidiary of Lockheed Martin Corporation, for the U.S. Department of Energy's National Nuclear Security Administration under contract DE-AC04-94AL85000.

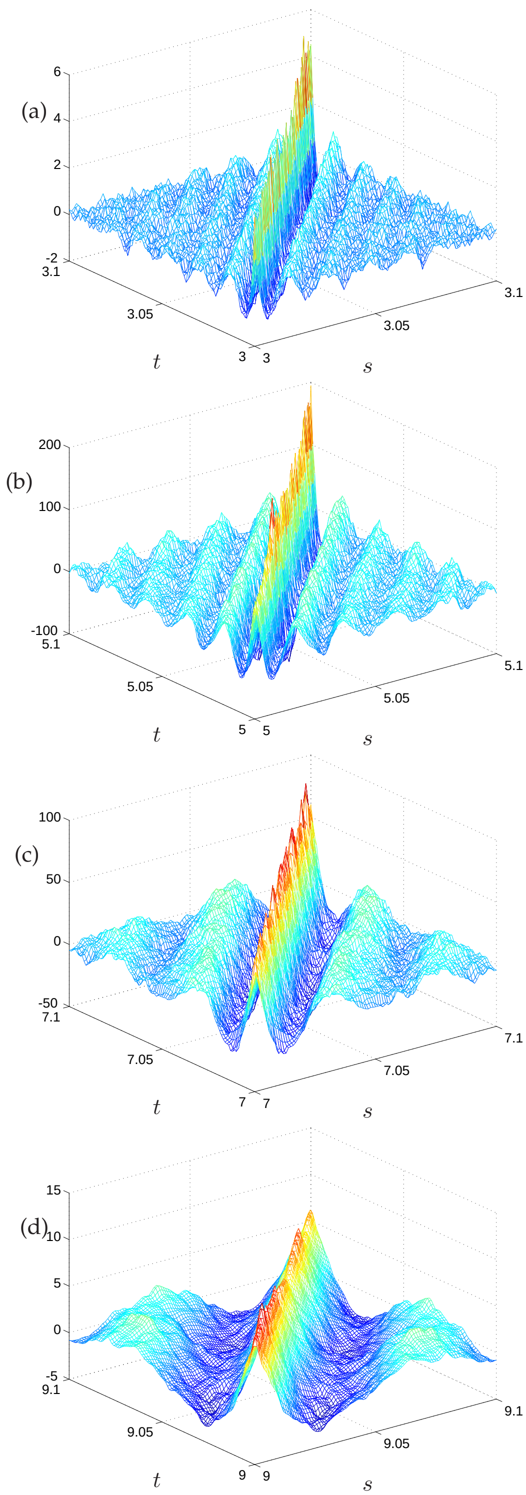

Fig. 7. Estimates of covariance function of $X(t)$ for various time segments during planetary entry. Units are in lb_f^2.

References

Yu. K. Belyaev, Analytic random processes, *Theory of Probability and its Applications*, 4(4):402–409, 1959.

J. S. Bendat and A. G. Piersol, *Random Data: Analysis and Measurement Procedures*, Second Edition, Wiley, NY, 1986.

J. L. Brown, On the error in reconstructing a non-band-limited function by means of the bandpass sampling theorem, *Journal of Mathematical Analysis and Applications*, 18:75–84, 1967.

J. L. Brown, On mean-square aliasing error in the cardinal series expansion of random processes, *IEEE Transactions on Information Theory*, IT-24(2):254–256, 1978.

W. Dieudonné and M. Spel, Entry probe stability analysis for the Mars Pathfinder and the Mars Premier Orbiter, *Proceedings of the International Workshop on Planetary Probe Atmospheric Entry and Descent Trajectory Analysis and Science*, October 6-9, 2003, Lisbon, Portugal.

P. Embrechts and M. Maejima, *Selfsimilar Processes*, Princeton University Press, Princeton, 2002.

R. V. Field, Jr., T. S. Edwards, and J. W. Rouse, Modeling of atmospheric temperature fluctuations by translations of oscillatory random processes with application to spacecraft atmospheric reentry, *Probabilistic Engineering Mechanics*, 26(2):231–239, 2011.

R. V. Field, Jr., M. Grigoriu, and C. R. Dohrmann, An algorithm for on-the-fly generation of samples of non-stationary Gaussian processes based on a sampling theorem, *Monte Carlo Methods & Applications*, 19(2):143–169, 2013.

J. N. Franklin, Numerical simulation of stationary and non-stationary Gaussian random processes, *SIAM Review*, 7(1):68–80, January 1965.

W. A. Gardiner, A sampling theorem for nonstationary random processes, *IEEE Transactions on Information Theory*, IT-

18:808–809, 1972.

P. A. Gnoffo, R. D. Braun, K. J. Weilmuenster, R. A. Mitcheltree, W. C. Engelund, and R. W. Powell, Prediction and validation of Mars Pathfinder hypersonic aerodynamic data base, *Proceedings of 7th AIAA/ASME Joint Thermophysics and Heat Transfer Conference*, AIAA-98-2445, June 15-18, 1998, Albuquerque, NM.

M. Grigoriu, Simulation of stationary processes via a sampling theorem, *Journal of Sound and Vibration*, 166(2):301–313, 1993.

M. Grigoriu, A class of non-Gaussian processes for Monte-Carlo simulation, *Journal of Sound and Vibration*, 246(4):723–735, 2001.

M. Grigoriu, *Stochastic Calculus. Applications in Science and Engineering*, Birkhäuser, Boston, 2002.

M. Grigoriu, A class of models for nonstationary Gaussian processes, *Probabilistic Engineering Mechanics*, 18(3):203–213, 2003.

M. Grigoriu, A spectral-based Monte Carlo algorithm for generating samples of nonstationary Gaussian processes, *Monte Carlo Methods & Applications*, 16(2):143–165, 2010.

H. D. Helms and J. B. Thomas, Truncation error of sampling-theorem expansions, *Proceedings of the IRE*, 50:179–184, 1962.

D. B. Hernández, *Lectures on Probability and Second Order Random Fields*, World Scientific, London, 1995.

A. J. Jerri, The Shannon sampling theorem - its various extensions and applications: A tutorial review, *Proceedings of the IEEE*, 65(11):1565–1596, 1977.

G. Y. Jumper, H. M. Polchlopek, R. R. Beland, E. A. Murphy, P. Tracy, Balloonborne measurements of atmospheric temperature fluctuations, *28th Plasmadynamics and Lasers Conference*, AIAA-97-2353, Atlanta, GA, 1997.

G. G. Justus and A. Woodrum, *Atmospheric Pressure, Density, Temperature and Wind Variations Between 50 and 200 km*, NASA Contractor Report NASA CR-2062, Washington, DC, May, 1972.

C. G. Justus, C. W. Campbell, M. K. Doubleday, and D. L. Johnson, *New Atmospheric Turbulence Model for Shuttle Applications*, NASA Technical Memorandum 4168, Washington, DC, January, 1990.

A. Papoulis, *Signal Analysis*, McGraw-Hill Book Company, New York, 1977.

A. Papoulis, Error analysis in sampling theorem, *Proceedings of the IEEE*, 54(7):947–955, 1966.

M. B. Priestley, Evolutionary spectra and non-stationary processes, *Journal of the Royal Statistical Society, Series B*, 27(2):204–237, 1965.

A. Weill, M. Aubry, F. Baudin, A study of temperature fluctuations in the atmospheric boundary layer, *Boundary-Layer Meteorology*, 10(3):337–346, 1976.